

# Constrained Path Optimization in G0 + Group Children Restraint System based on UN R129

Leyuan PENG<sup>1</sup>, Yong HAN<sup>1,2</sup>, Di PAN<sup>1</sup>, Koji Mizuno<sup>3</sup>

1. Xiamen University of Technology, Xiamen, China, 361000, yonghanxmut@gmail.com
2. Third military medical university traffic institute for medical research, Chongqing, China, 404100
3. Nagoya University, Nagoya, Japan, 4648603

**Abstract:** The Q1 dummy FE model was used to analyze different restraint paths of a G0+ group of CRS based on UN R129 rear facing sled test method. Four difference seatbelt restraint paths of the rear facing CRS were analyzed and the displacement of the CRS and physical injury parameters of Q1 dummy were compared. The results showed that the head maximum displacement of Q1 dummy was reduced by 35.05 mm and chest resultant acceleration was reduced by optimizing the constraint path of the backward restraint system. This paper provides a reference for design and development on G0+ group of child restraint system in the future.

**Key words:** child restraint system; constraint path; frontal impact; finite element simulation

## 1 Introduction

Traffic accidents are an important source of casualties among Chinese children. There were 2690 children dead in the Chinese traffic accidents in 2010, accounting for 39.3% of the total deaths among urban children <sup>[1]</sup>. However, according to the National Highway Traffic Safety Administration (NHTSA) statistics, the number of deaths under the age of 15 was 714 in 2014 <sup>[2]</sup>. Compared with the United States, the death rate of China's children in the traffic accident is very high. The relevant data shows that the child's own special body structure determines the child occupant to need higher protection requirements in collision process <sup>[3]</sup>. Arbogast K B et al. <sup>[4]</sup> pointed out that the child occupants less than 40 pounds should use the child restraint system; The CRS installed backward can play a good support and protection when the weight is less than 13 kg <sup>[5]</sup>; QI <sup>[6]</sup> studied the injury analysis of different fixation methods of the backward restraint system and concluded that the dummy's injury criteria is optimal in the ISOFIX fixed; Mizuno et al. <sup>[7]</sup> analyzed kinematics response and chest acceleration of the Leaman Eurobegin RF CRS in the JNCAP and ECE base test and concluded that the chest acceleration in the ECE base test increased earlier.

Based on the UN R129, this study established the frontal impact sled test simulations model of the G0 + group of CRS with four different seatbelt restraint paths. The optimal constraint path is analyzed by the single factor test design method, which is helpful to improve the protective performance of G0 + group of CRS.

## 2 Methodology

### 2.1 Finite Element Model

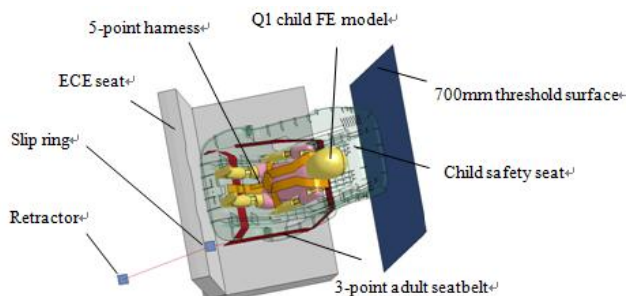


Figure 1. Rear facing CRS frontal impact simulations model

In this paper, the frontal impact FE model based on UN R129 is shown in Fig. 1. The FE model includes Q1 child finite element model, ECE test seat, child safety seat, 5-point harness, 3-point adult seatbelt, retractor, slip ring. The

ECE test seat FE mode is modeled by hexahedral element. The CRS adopts the positive design method to carry on the geometric modeling and the mesh division, which total mass of 4.59kg, element number of 24397, node number of 22817.

## 2.2 Material Test

The skeleton of CRS is mainly made of plastic PP, and the curve (Fig. 2) used in the simulation is the true stress - strain curve in the shaping stage. Q345 is used in the bottom guide groove which 3-point adult seatbelt passed. See Table 1 for additional material properties

Table 1. Material properties

|          | Component    | Material Type               | Elastic Modulus /MPa | Poisson's ratio | Density /(kg m <sup>3</sup> ) |
|----------|--------------|-----------------------------|----------------------|-----------------|-------------------------------|
| CRS      | skeleton     | Piecewise Linear Plasticity | 1050                 | 0.3             | 920                           |
|          | guide groove | Q345                        | 210000               | 0.3             | 12000                         |
| ECE seat | cushion      | Low density foam            | 0.1                  | —               | 43                            |

## 2.3 Test Conditions

In the UN R129, the frontal impact test for the rearward-facing CRS requires a sled speed of  $50 \pm 2$  km/h, the test stop distance is  $650 \pm 50$  mm. The acceleration inputted in the simulation is shown in Fig. 3.

## 2.4 Simulation Results Analysis

The maximum head excursion (Table 2) with constraint path before the improvement is 644.04 mm. The seat is optimized by changing seatbelt restraint path because of the big head excursion.

Table 2. The injury Criteria Before improvement

| Injury Criteria    | HPC* (15) | Head acceleration 3ms/g | Head excursion/mm | Chest acceleration 3ms/g |
|--------------------|-----------|-------------------------|-------------------|--------------------------|
| Regulations        | 600       | 75                      | 700               | 55                       |
| Before improvement | 218.4     | 47.8                    | 644.08            | 66.1                     |

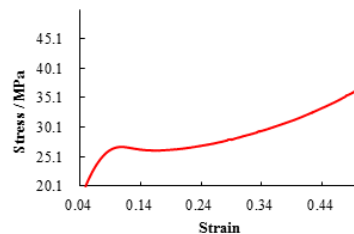


Figure 2. The true stress - strain curve of PP

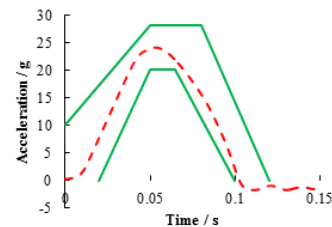


Figure 3. The acceleration curve

## 3 Optimization

### 3.1 Seatbelt Restraint Path

It found that the seatbelt restraint path of CRS plays an important role in improving the head displacement. Therefore, this paper modeled three restraint paths to analyze the kinematic response and injury criteria of dummy shown in Fig. 4:

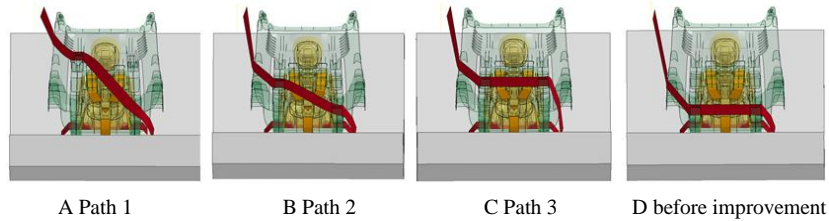


Figure 4. The improved constraint path

### 3.2 Occupant Kinematics

Fig. 5 and Fig. 6 show the kinematic and the trajectory of Q1 dummy in the X-Z plane. The child occupant started with a significant kinematic response from 50ms, and then moving a distance upwardly along the seatback frame. Compared with Fig. 7, we can find that the maximum head displacement achieved at about 70ms-80ms and the head displacement of path 1 is the smallest, which is consistent with the trajectory of the dummy head centroid in the X-Z plane in Fig. 6.

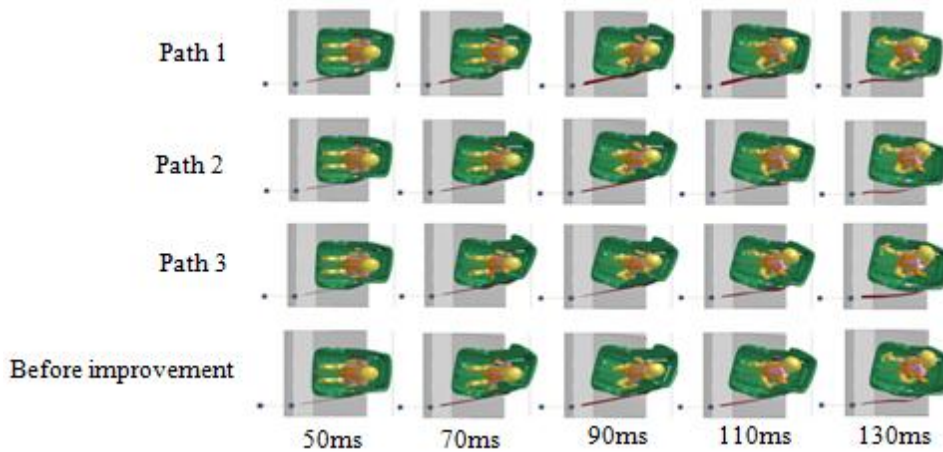


Figure 5. Dummy kinematic

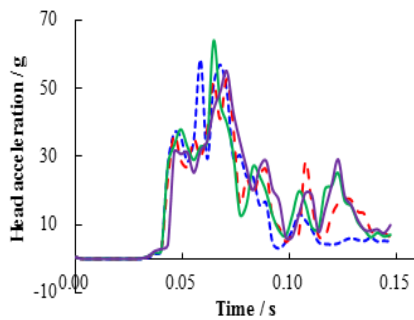


Figure 8. The head acceleration

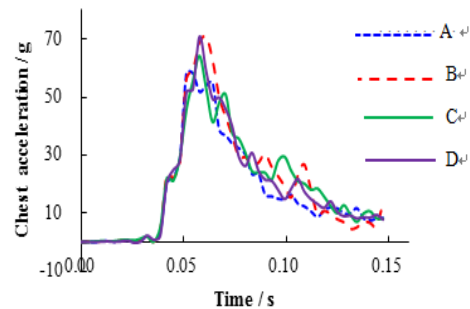


Figure 9. The chest acceleration

Table 3. Injury Criteria

| Injury Criteria    | HPC* (15)   |           | Head excursion/mm |      | Head acceleration 3ms/g |           | Chest acceleration 3ms/g |           |
|--------------------|-------------|-----------|-------------------|------|-------------------------|-----------|--------------------------|-----------|
|                    | Regulations | 600       | 700               | 75   | 55                      | 3ms       | 55                       |           |
|                    | value       | time      | maximum           | time | 3ms                     | time      | 3ms                      | time      |
| Path 1             | 240.9       | 57.4—72.4 | 609.3             | 70   | 48.6                    | 65.9—69.5 | 58.7                     | 51.2—54.2 |
| Path 2             | 238.1       | 56.7—71.7 | 622.16            | 74   | 44.2                    | 67.7—71.9 | 70.4                     | 57.9—60.9 |
| Path 3             | 216         | 56.7—71.7 | 618.21            | 84   | 44.8                    | 63.1—67.6 | 60.4                     | 56.5—59.5 |
| Before improvement | 218.4       | 59.6—74.6 | 644.08            | 79   | 47.8                    | 70.2—73.2 | 66.1                     | 56.8—59.8 |

### 3.3 Injury Criteria

The head result acceleration and the chest result acceleration are shown in Fig. 8 and Fig. 9, and injury criteria is given in Table 3. In the simulation, chest acceleration will always be a peak before the head acceleration<sup>[8]</sup>. Compared Fig. 8, Fig. 9 and Table 3, the path 1 is optimal.

### 4 Validity Verification of Optimal Constrained Path

Fig. 10 shows the comparison of occupant kinematics of the experiment and simulation. The maximum displacement of the head is 615.01mm in the test, the simulation is 609.03mm, which is lower than the experimental value 0.97%; The comparison of chest result acceleration is shown in Fig. 11. The trend of two curves is basically the same. The peak of chest acceleration was 59g in the test, which of simulation was 62g, the difference was 5.08%. The deviation between the experimental value and the simulated value does not exceed 15%<sup>[9]</sup>, so the optimal path FE model is valid.

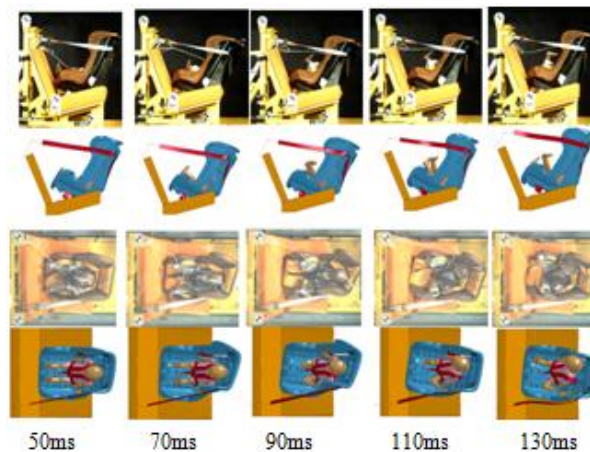


Figure 10. The comparison of occupant kinematics of the experiment and simulation

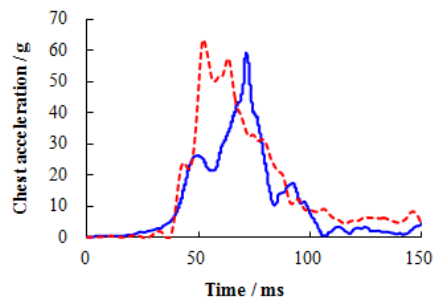


Figure 11. The comparison of chest result acceleration

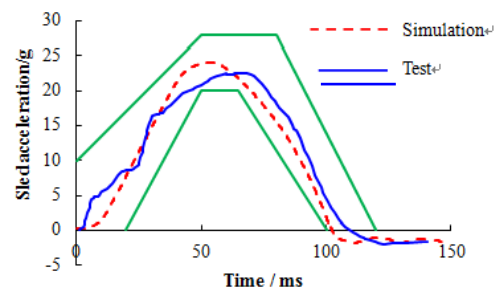


Figure 12. The comparison of sled acceleration

### 5 Discussions

There are some reasons why chest result acceleration is different in the test and simulation:

1. The sled acceleration curve (Fig. 12) used in the test and simulation is different;
2. The dummy is not the same, which of the test is P1.5 and the simulation is Q1;
3. To simplify the model, the simulation used only skeletons, ignoring the cloth cover and baby liner that playing a buffer role in the actual test.

### 6 Conclusions

Through the above analysis, we can draw the following conclusions:

1. By optimizing the restraining path of the rearward-facing CRS, the head maximum displacement is reduced by 35.05mm, and the chest acceleration resultant was reduced.

2. The installation of optimized constraint path is more convenient, to a certain extent, reducing the probability of misuse.

## Acknowledgements

The authors would like to acknowledge support of the National Natural Science Foundation of China (Project No: 31300784, 51675454), the Natural Science Foundation of Fujian Province, China (Project No: 2016J01748) and the Outstanding Youth Scientific Research Program of Fujian Province, China.

## References

- [1] ZHANG Jinhuan, ZHANG Xiong, XIAO Lingyun, et al. Experimental studies on safety when child restraint system (CRS) misused[J]. J Automotive Safety and Energy, 2014, 5(01): 30-37. (in Chinese)
- [2] National Highway Traffic Safety Administration. 2014 Traffic Safety Factsheet CHILDREN. <http://www.nhtsa.dot.gov/2016-05>.
- [3] Cao Libo, Zhang Ruifeng, Liu Yao. Study on the Child Passenger Injury Mechanism and Protection Measures[J]. Chinese Journal of Automotive Engineering, 2012, 2(1): 16-23. (in Chinese)
- [4] Arbogast K B, Durbin D R, Cornejo R A, et al. An evaluation of the effectiveness of forward facing child restraint systems[J]. Accident Analysis & Prevention, 2004, 36(4): 585-589.
- [5] GUAN Guopeng. The simulation analysis and test study of multi-functional child-safety chair[D]. Changsha: Hunan University , 2013. (in Chinese)
- [6] QI Xiangcui. The child restraint system in frontal impact simulation research on correct use and misuse [D]. Changsha: Hunan University, 2011.(in Chinese)
- [7] Mizuno K, Ikari T, Kawahara H, et al. Effect of test conditions on child occupant responses in CRS[J]. International Journal of Automotive Engineering, 2011, 2(2): 26-32.
- [8] YANG Xingmei. A study of child occupant injury protection from passenger car collisions [D]. Changsha: Hunan University, 2010.(in Chinese)
- [9] HAN Yong, XIE Jinping, et al. Parameter optimization of CRS seatbelt constrain paths based on design-of-experiment (DOE)[J]. J Automotive Safety and Energy, 2015, 6(03): 230-236.